

PLANETARY NEBULAE IN THE BULGE

Albert Zijlstra and Paul Ruffle

UMIST, Department of Physics, P.O. Box 88,
Manchester M60 1QD, UK.
a.zijlstra@umist.ac.uk

Krzysztof Gesicki

Centrum Astronomii UMK, ul.Gagarina 11,
PL-87-100 Torun, Poland

1 Bulge PNe

The PN population in the Bulge is the only sample of Galactic PNe with known, uniform distances, and is close enough that the nebulae can be resolved. In addition, the progenitors are known to be old, low-mass stars. This uniform population with well-known distance is well suited to statistical study of topics such as: the origin of morphologies and relation to stellar progenitors; enrichment history of the Bulge; and the initial-final mass relation.

The observational database for Bulge PNe is still far from complete. Even elementary data such as diameters is often not or only poorly known. We have initiated a large observational survey of Bulge PNe, to obtain imaging and spectroscopy for all known Bulge PN. Imaging data yield: (1) diameters (already known for less than half the sample); (2) absolute fluxes for images in emission lines, to typical accuracy of 5–10%; (3) morphologies, for objects large enough to be well resolved; (4) stellar magnitudes and Zanstra temperatures, again for well resolved objects. High resolution spectroscopy gives information on the internal velocity fields, dynamical ages and stellar mass.

2 Images

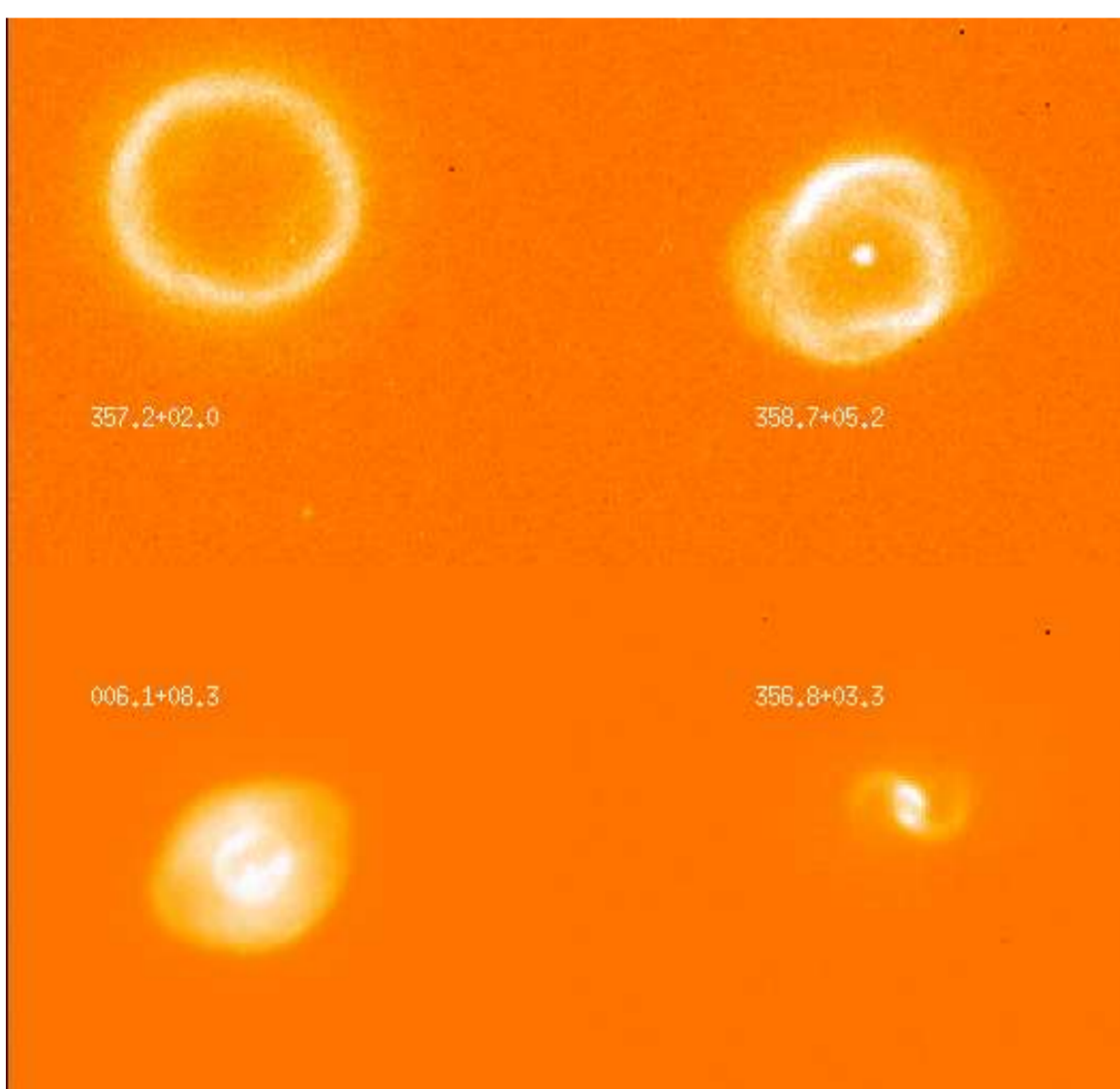


Figure 1: Four $H\alpha$ HST images of Bulge PNe. All four are on the same scale: 357.2 ± 0.2 is $3''$ in diameter.

Objects larger than 4 arcsec can be well resolved in good seeing from the ground. For small objects, HST imaging is required and a snapshot imaging programme with WFPC2 has been carried out in Cycle 11. About 200 larger objects have been observed with the NTT.

Example HST images of Bulge PNe are shown in Fig. 1. The most extreme morphology is shown by the most compact object. The objects shown are unlikely to show an evolutionary sequence. The images provide some support for the suggestion that bipolarity is related to slower expanding, dense torii.

Example NTT images are shown in Fig. 2.

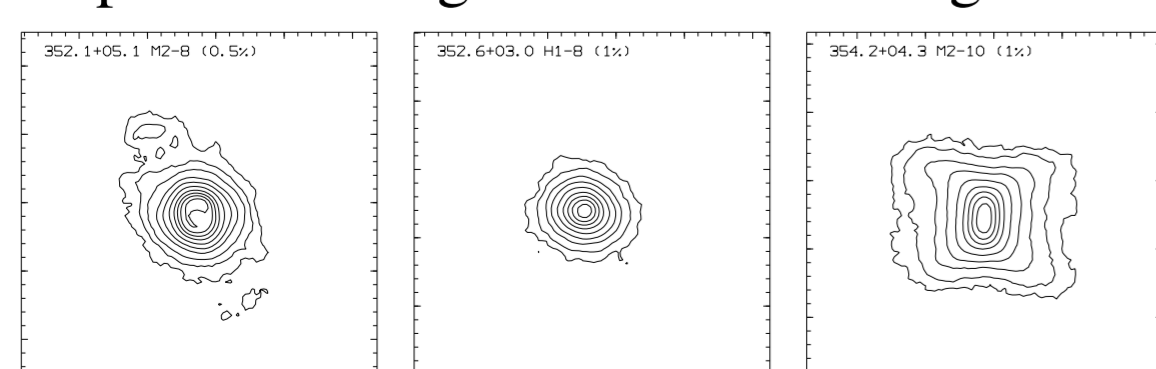


Figure 2: Example $H\alpha$ NTT images. Each box is 26 arcsec on a side.

3 Velocity fields

The expansion velocity of a PN can be measured from the line widths, after correcting for thermal broadening. [NII] lines tend to show larger width than the higher excitation [OIII] lines, showing that the outer layers expand faster.

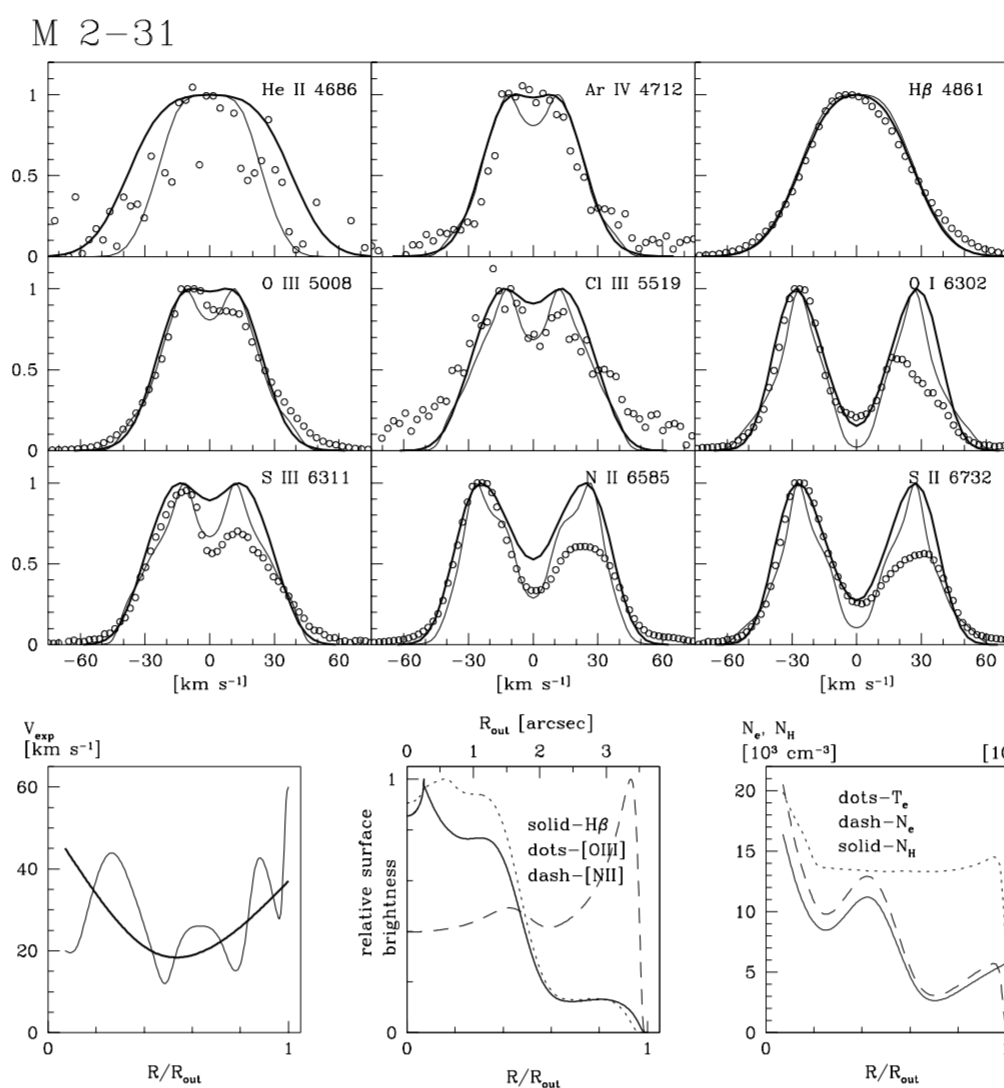


Figure 3: Profile fitting an velocity field for M2-31.

We calculate expected line profiles from photoionization models using an assumed velocity field, convolving with the slit parameters. If a range of lines with different excitation energy is available, a detailed radial velocity field can be determined. We apologize for spherical symmetry. An example is shown in Fig. 3, for the [WC] Bulge PN M2-31. The bold line in the lower left panel shows the preferred field: it shows acceleration at the inner and outer radius. We find inner acceleration to be common among PN. The fit requires a turbulent component to the velocity: without this, the thin line is obtained. Turbulence is found mainly for [WC] PN.

We have obtained about 150 echelle spectra for Bulge PNe. They are less deep than the one shown in Fig. 3 but cover at the minimum [OIII], [NII], $H\alpha$ and $H\beta$. Other lines are often also detected. The velocity fields to be derived from this will be used in the interpretation of the HST and NTT images. The goal is to determine evolutionary sequences.

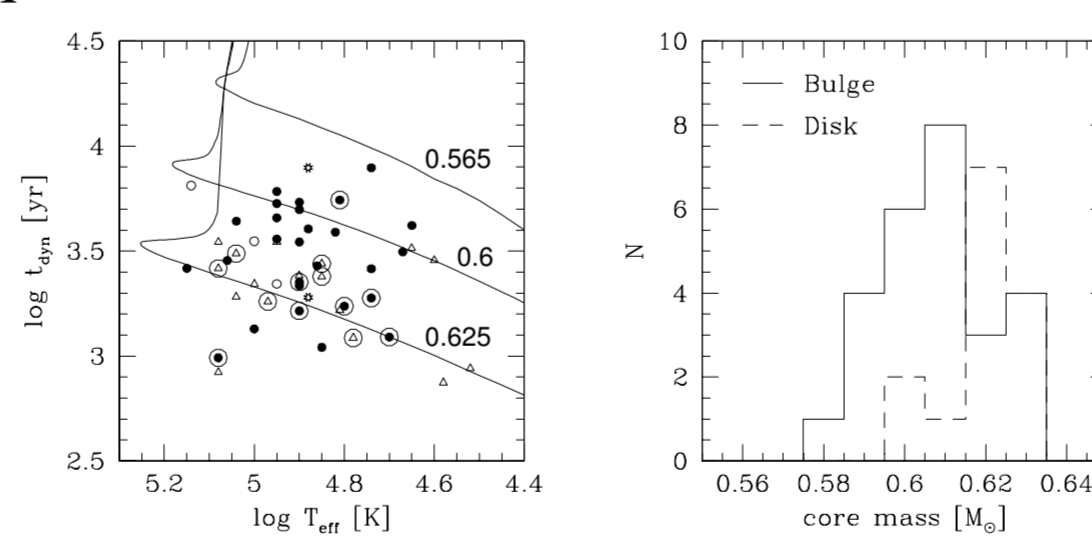


Figure 4: Left: stellar temperature versus dynamical age. Evolutionary tracks are shown superposed. Right: Core masses derived from the left panel.

If both the expansion velocity and the diameter are known, a dynamical age can be calculated. We make corrections for the slower expansion during the pre-PN phase and the non-uniform velocities. The resulting age can be compared with the temperature of the central star. The time scale for the temperature increase of the star should be the same as the time scale for the nebulae expansion. This is the most sensitive technique to measure relative stellar masses. Fig. 4 shows the result for a sample of Bulge and Disk PNe. Very similar core masses are obtained for both groups.

4 Extinction

The extinction towards a PN can be determined in two ways: the hydrogen line ratios, and the ratio between the radio flux and hydrogen line flux. The former measures the reddening and the latter the absolute extinction. Standard reddening laws are used to relate the two two measurements. Radio fluxes come primarily from VLA surveys. We do not use 6-cm fluxes below 10 mJy, which have been shown to be less reliable. The $H\alpha/H\beta$ decrement is taken from the ESO-Strasbourg catalog. The decrement is normally measured from a single spectrum and is therefore less affected by flux calibration errors. The catalog also lists absolute line fluxes. We can measure these from our background-subtracted narrow-band images. Comparison shows that the catalog values have large uncertainties, of 0.2-0.4 dex (Fig. 5).

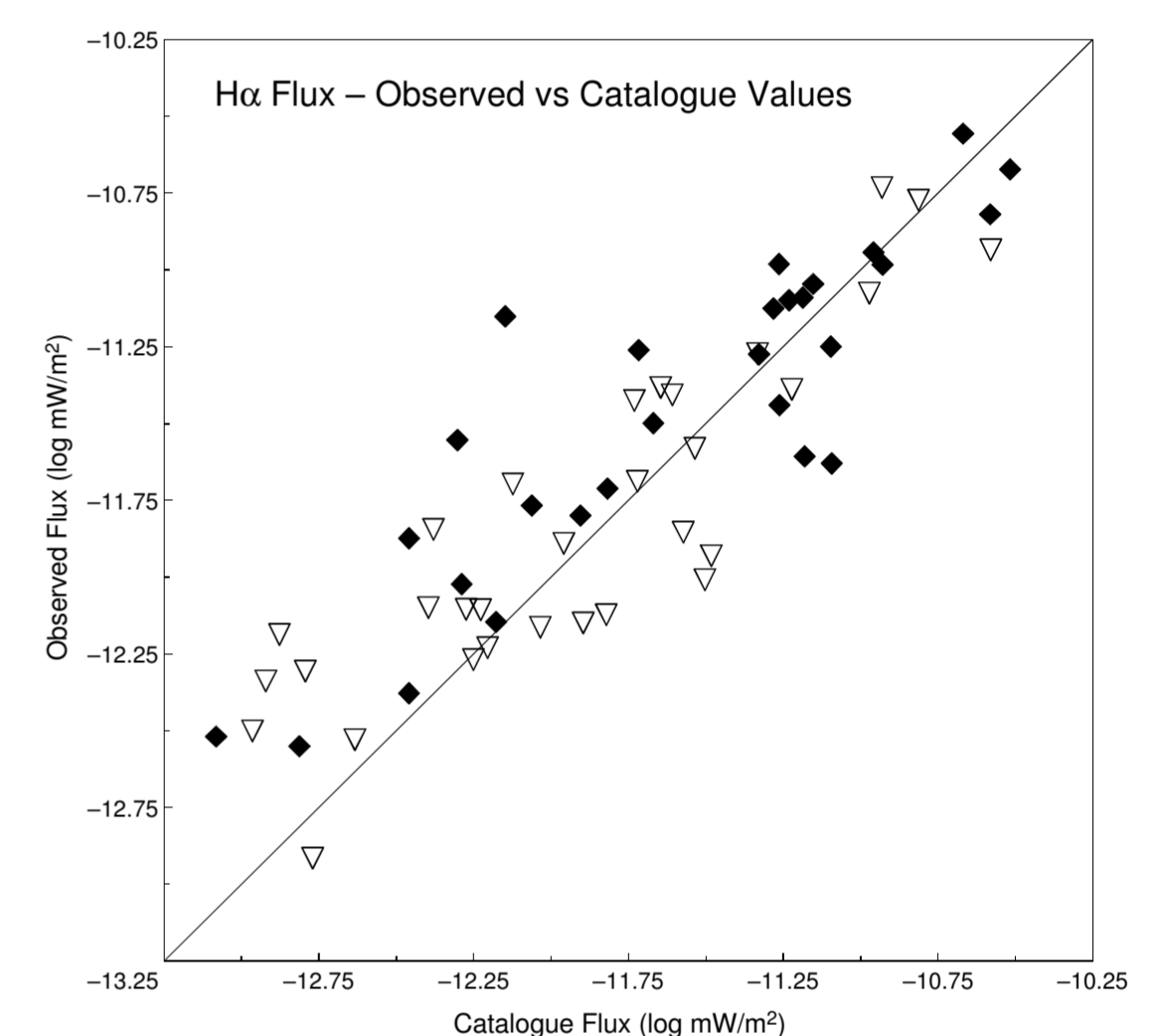


Figure 5: Our $H\alpha$ flux versus values listed in the catalog.

Fig. 6 shows a large discrepancy between the extinction derived from the radio/ $H\alpha$ flux, versus the one derived from the Balmer decrement. The two can be reconciled if we assume a steeper reddening law: in terms of $R_V = A_V/E(B-V)$, a value significantly lower than the 'universal' $R = 3.1$ is implied. We find an average value of $R_V = 1.8$. Values of 1–1.5 are found for the objects with the lowest extinction. Higher extinction objects show R_V up to 2.5.

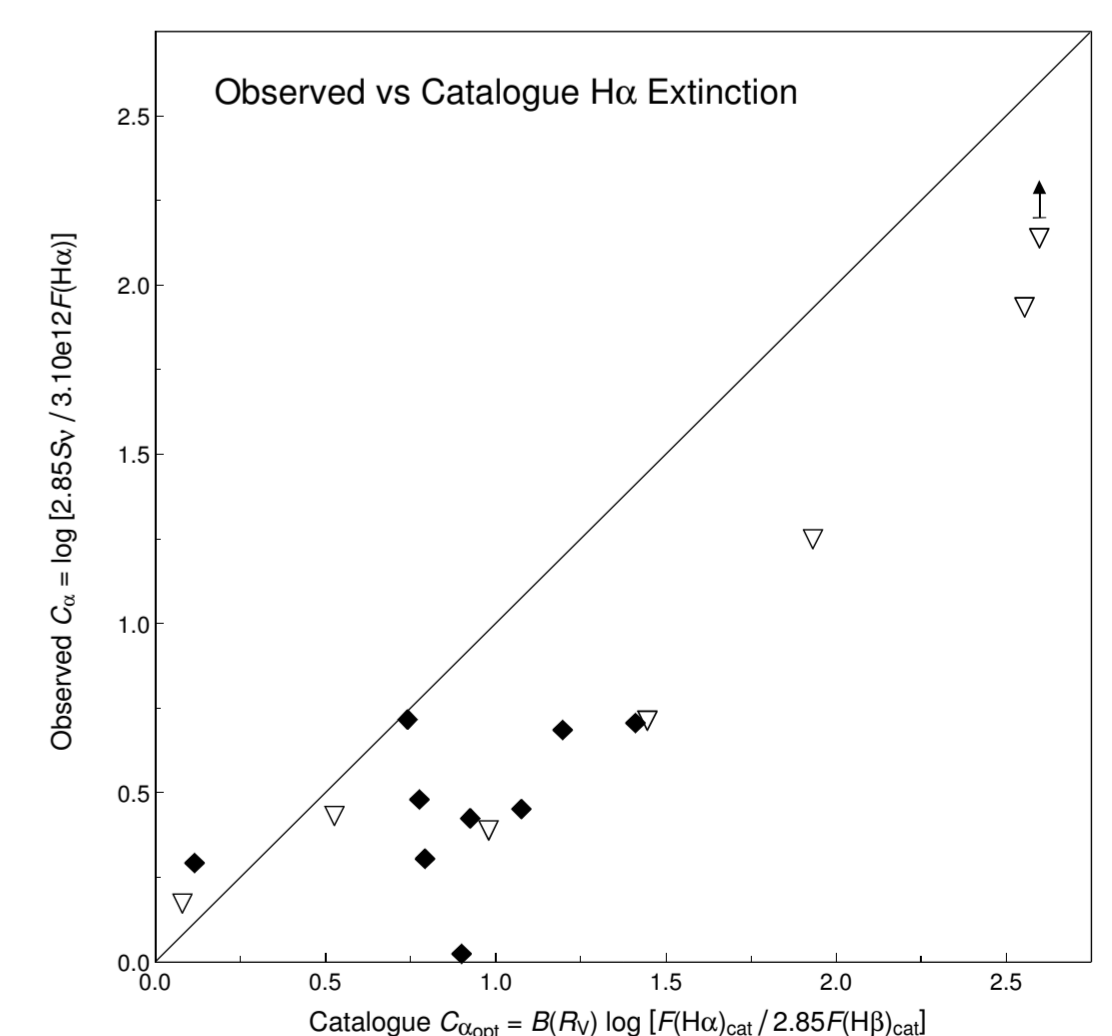


Figure 6: radio extinction versus Balmer decrement extinction, for Bulge PNe with accurate radio and $H\alpha$ fluxes.

The anomalous extinction may be attributed to the high supernova rate in the inner Galaxy. Supernova shocks can reduce the size of the dust grains in the Warm Ionized Medium, located above and below the Disk. This WIM dominates the lines of sight towards known Bulge PNe.